A SELF-SUSTAINED BATTERY-LESS MEMS BASED SENSOR NODE THROUGH FAR FIELD WIRELESS POWERING

[1]M. KUMARASAMY RAJA, [2]YAN DAN LEI, [3]SALAHUDDIN RAJU

Institute of Microelectronics, A*STAR, Singapore
E-mail: raja@ime.a-star.edu.sg

Abstract - This paper details on the sensor nodes (SNs) for aircraft surface sensing, especially operating them on the far-field wireless powering, also known as RF powering. The SNs includes RF energy harvesting circuit, harvesting voltage booster, data link transceiver and sensor interface circuits. Modelling & Simulation of the most critical block in the link, RF-DC converter is described. The RF-DC converter exhibits more than 25% efficiency even with the input power levels less than -18dBm. Thus, without exceeding the FCC emission limits, the base station is able to wirelessly power the SNs up to 10 m range.

Keywords - Battery-less sensor nodes, Wireless charging, Far filed RF energy harvesting

I. INTRODUCTION

Existing sensor nodes (SN) for Aircraft surface sensing, have successfully avoided the bulky cables (in the earlier solutions) which were also not maintenance friendly as the repairs usually lead to re-certification issues. Yet, the replacement of battery has become a significant maintenance hassle, in terms of accessing the location of SNs and following the disposal procedures. Also the current battery-less SAW resonator based solutions does not support efficient uploading of critical sensor data on demand and the additional loss in the resonator results in lower range.

In this paper we demonstrate the SN and BSU which enables battery-less operation of SN resolving the battery replacement hassles and enables communication of critical sensor data on demand similar to the wireless sensor networks (WSN) in Industry/Home automation applications. In the absence of battery, the SNs are powered by far field RF powering. Range is improved compared SAW based solutions due to reduced path loss since, the signal travels only one way and there is no resonator loss.

The Sensor Node will be realized using components of the shelves (COTs) devices for both Energy Harvesting and wireless link. Thus prototyped SN will be tested with an interrogator (also called reader or BSU), for far-field RF powering and wireless data transfer.

The data link transceiver selection will be in concurrence with the reader development. Majority circuits of the whole SN can be integrated into an IC and hence the SN with an aggressive form factors can be realized. Since the low power radios like Bluetooth and zigbee [1] can cover 10s of meters, the main challenge and critical path is wireless powering for 8- 10m range. We demonstrate the feasibility of the far-field RF powering, by (i) charging the super cap through the RF signal from BSU and by (ii) operating the SN from thus harvested energy. In this paper, we detail the selection of frequency band and the modelling and simulation of the far-field RF powering link and the power budgeting for the SN.

II. SYSTEM ARCHITECTURE DESCRIPTION

The Sensor note (SNS) includes RF energy harvesting circuit (RF-DC), voltage booster or Power management, low power transceiver (TxRx) for the data link and sensor interface circuits to sense the data as shown in Figure 1 below.

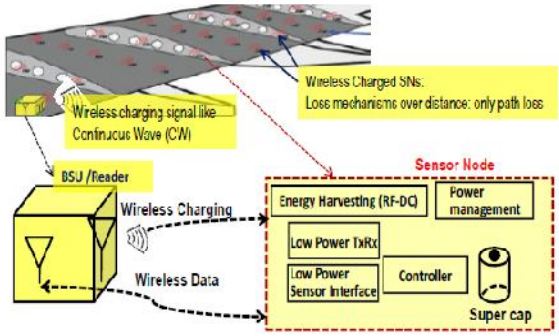


Figure 1: System diagram of the wirelessly powered wireless sensor network for aircraft surface sensing

2.1 Targeted Specifications

- BSU to power SN up to 8-10m range
- Simultaneous-operation of two links with ability bidirectional communicate control commands /requests for charging through data link
- Priority based critical data update without latency
- COTs SN size 6cm×4cm

Popular WSN wireless transceiver protocols like Bluetooth and Zigbee can achieve up to 100meters. The bottleneck in range comes from wireless charging as we need significant power (about -15dBm at least) to charge the SN. This is much higher than the sensitivity of wireless transceivers (about -95dBm). Hence, the path loss in the air

assumes importance. As the path loss depends on the frequency band, a Pugh matrix was made to make the choice of frequency as seen in next section. Other parameters such as availability of components and interference with data communication was also checked.

2.2 Choice of Frequency band

The choice of wireless powering frequency from one of the ISM band is made considering various factors. In the Pugh matrix below (Table I) 2.5 GHz band was assumed for data communication purpose. Considering all the factors, as shown in the table, 900 MHz is selected for the prototyping. It should be mentioned here that, the low power transceiver and or the energy harvesting circuit can be integrated into an IC for miniaturizing the SN. We can also be more selective on the frequencies based on the application need and ideal performance rather than restricted by available COTS components.

Table 1: Pugh Matrix for frequency band selection for far field RF powering (2.4GHz band assumed for data link)

Pugh Selection for frequency band (MHz)					
Criteria ↓	**Priority**	**430**	***900***	**2450**	**5250**
(Path) Loss	**8**	2	*1*	0	0
COTs Size & Availability	**7**	0	*2*	2	1
Interference	**8**	2	*2*	0	2
Potential applications	**4**	-	*s*	+	s
Net Weighed Merit	-	**32**	***42***	**18**	**27**

2.3 Simulation of RF-DC converter

The wireless energy harvesting (EH) circuit at the sensor node consists of the antenna, RF-DC converter, power management circuit which charges the super capacitor. The RF-DC converter is the critical block in the EH path. Figure 2 shows the RF-DC converter. While the LC circuit at the input (left) performs impedance matching function, the two diodes with the capacitor execute the core task of converting the RF to DC.

Non-linear nature of the diode, which is the main component converting RF to DC, makes its impedance to vary with the input signal level. In order to maximize the harvested DC, Z11 as shown in figure 2, which is the input impedance including the matching network is to be optimized such that maximum voltage appears at the input.

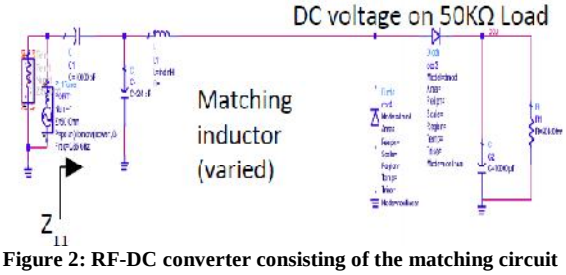


Figure 2: RF-DC converter consisting of the matching circuit and the doubler.

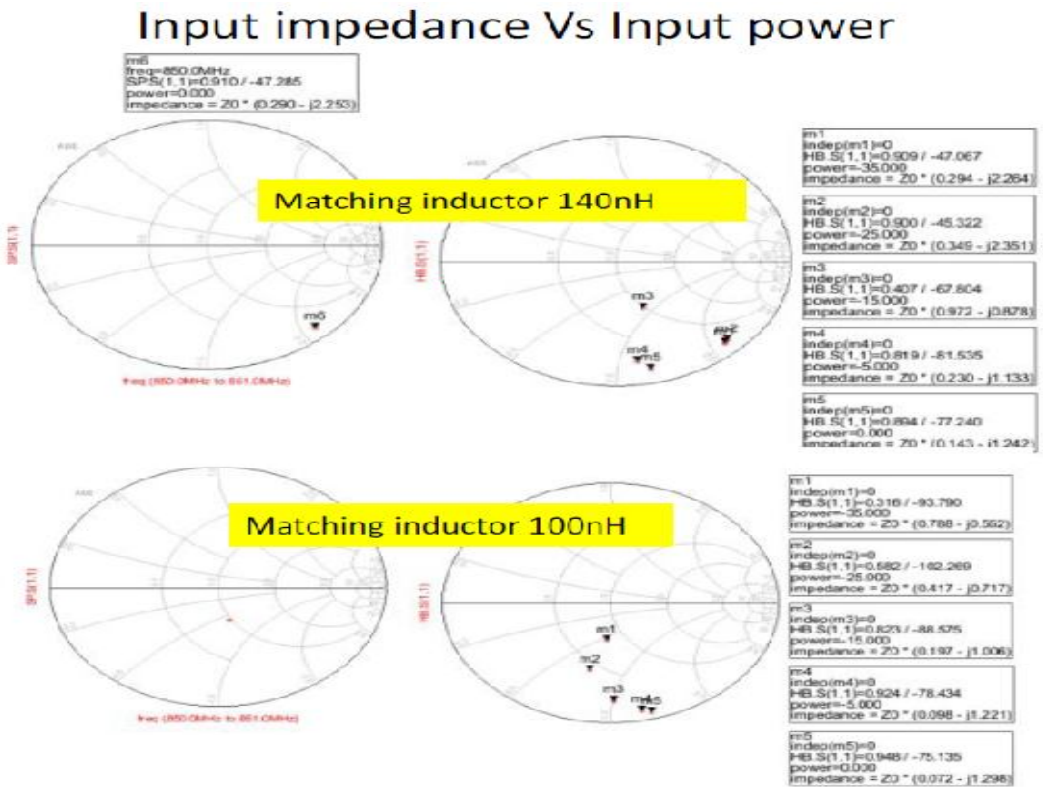
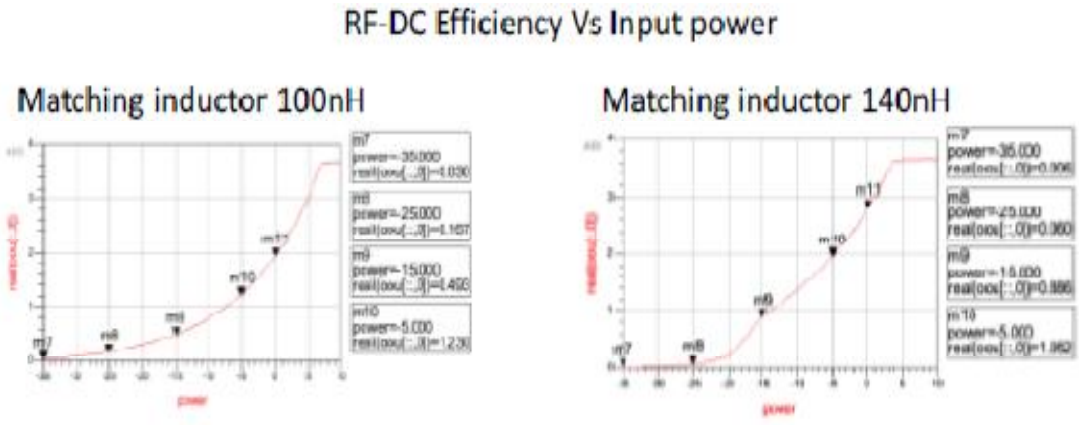


Figure 3: Simulated input impedance (Z11) with input power varied.

In figure 3, the left side smith chart shows the small signal impedance and the right side shows the large signal impedance. With 140nH inductor, the impedance for higher power (>-15dBm) are placed near 50-Ω (mid-point), while for lower power the impedance is farther. In case of 100nH, there is no significant difference in impedance for low and higher power even though slightly away from 50-Ω.



Input power		Matching Inductance = 100nH				Matching Inductance = 140nH			
dBm	mW	Impedance	Output voltage	Output power mW	RF-DC Efficiency %	Impedance	Output voltage	Output power mW	RF-DC Efficiency %
Small signal		47.5-j29.5	-	-	-	14.5-j112.7	-	-	-
-35	0.0003	39.4-j27.6	0.03	1.8E-05	6.0	14.7-j113.2	0.006	7.2E-07	0.2
-25	0.0032	20.9-j35.9	0.167	5.6E-04	17.4	17.4-j117.6	0.06	7.2E-05	2.3
-15	0.03	9.85-j50.3	0.493	4.9E-03	16.2	48.6-j43.9	0.886	1.6E-02	52.3
-5	0.3	4.9-j61.05	1.23	3.0E-02	10.1	11.5-j56.65	1.952	7.6E-02	25.4
0	1	3.6-j64.9	1.95	7.6E-02	7.6	7.15-j62.1	2.816	1.6E-01	15.9

Figure 4: Simulated RF-DC efficiency with input power varied.

Simulated input impedance (Z11) in figure 3, with input power varied, demonstrates the variation in (large signal) Z11. The small signal Z11 is shown at the left for reference. With 140nH inductor, the impedance for higher power (>-15dBm) are placed near 50-Ω (mid-point), while for lower power the impedance is farther. In case of 100nH, there is no significant difference in impedance for low and higher power even though slightly away from 50-Ω. How this impedance affects the RF-DC efficiency can be seen from Figure 4, Simulated RF-DC efficiency with input power varied. Notice that for higher power levels the advantage of 140 nH inductor is significant as the increased impedance as shown in figure 3 improves the dc output. In case of 100nH, there is no significant transition in efficiency and the curve is smooth as foreseen by impedance in figure 3. Hence the inductance needs to be lowered at very low power levels. Notice that for higher power levels the advantage of 140nH inductor is significant as the increased impedance as shown improves the dc output. In case of 100nH, there is no significant transistion in efficiency and the curve is smooth as foreseen by impedance in figure 3.

The objectives of this work are, (i) COTs based compact SN prototype of size 6cm×4cm, and functional demonstration and (ii) Novel Design of high RF-DC conversion efficiency (>30%) at low received RF power (<-18dBm). The simulated efficiencies at - 18dBm with the 140nH inductor is slightly less than the targeted 30% (27% approximately). Novel techniques were explored further to attain the targeted efficiency of 30%. One of the technique with closed loop control is shown in Figure 5 below. Varying the inductor and varying capacitor will be explored according to the input power.

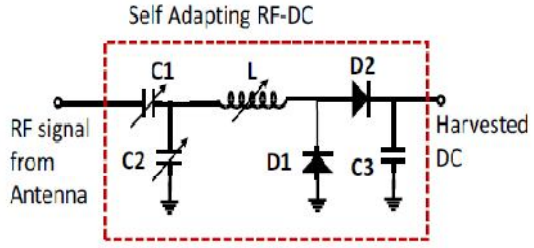


Figure 5: Proposed adaptive technique to achieve optimal RF-DC efficiency across wider dynamic range

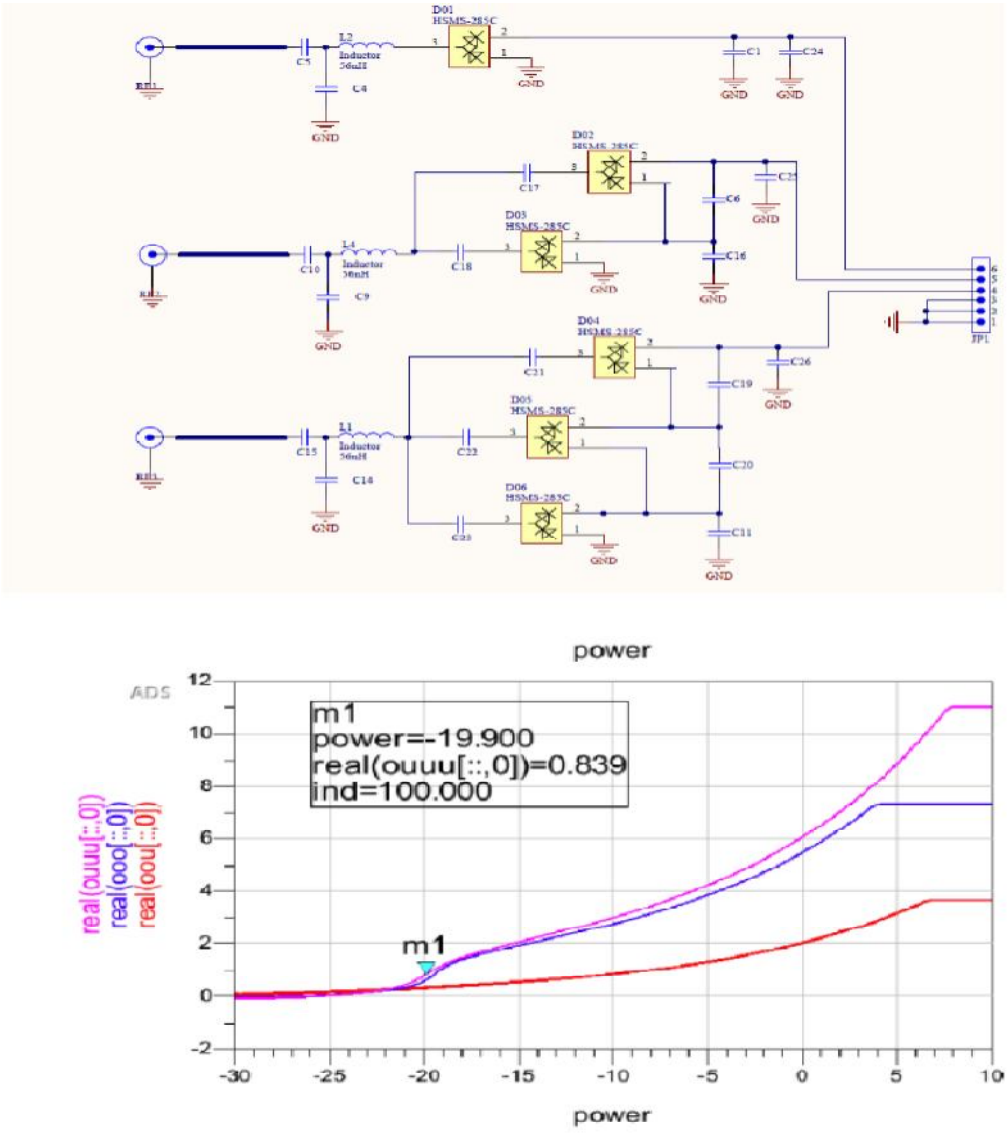


Figure 6: (a) Schematics showing 1,2,3 stages of doubler circuits with LC matching in front and (b) corresponding simulated results

2.3.2 Results of RF-DC

In order to evaluate the energy harvesting circuit performance, 1,2,3 stages doubler circuits are drawn as shown in Figure 6(a). The simulation of Effect of number of stages on the output voltage of energy harvesting circuit as shown in Figure 6(b).

The final fabricated PCB of our proposed energy harvesting is shown in Figure 7. The PCB is fabricated with FR-4 substrate and has two layers, one of which serves as a ground plane. The prototype consists of the design obtained from the proposed optimization. We select components with values and ratings of their performance parameter as close as possible to ones obtained from the simulation.

We validated the simulation results by testing the PCB with RF power from signal generator instead of the receiving antenna. Preliminary measurements show that DC power of 23.9µW could be harvested from -10dBm (100µW) RF (received) continuous wave (CW) power, yielding an efficiency of 23.9%.

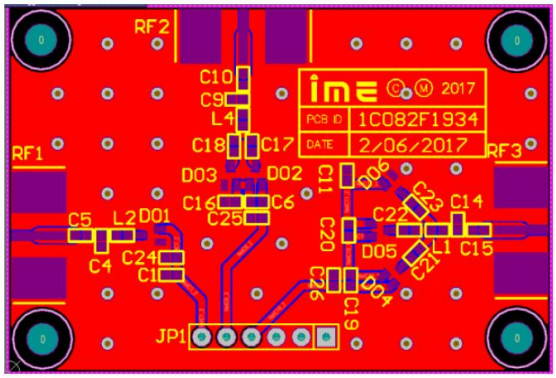


Figure 7: PCB for circuits of RF-DC converter.

SUMMARY

Self-sufficient operation sensor nodes (SNs) for aircraft surface sensing, by far-field wireless powering (also known as RF powering) is demonstrated. This report budgeted the block level specifications, choice of frequency bands to achieve self-sufficient operation. Simulated results of the

most critical block (RF-DC), appearing in the most critical RF powering link. Achievable simulated efficiency is only 45% at -16dBm input power, which is slightly lower than targeted 50%. Primitive RF-DC converter was verified by measurement. The efficiency at -10dBm RF power is 23.9% which is enough to operate the SN and transmit 15 seconds in 20 minutes, which is more than enough for a SN. With power beaming and efficiency enhancement, our target of >50% efficiency will be explored in the subsequently.

ACKNOWLEDGMENTS

The authors thank Subodh Kumar Keshri and Dale King of Airbus for the technical discussions. The authors also are thankful to A*STAR Aerospace Programme (AP) for the support.

REFERENCES

[1] M.Kumarasamy Raja, Xuesong Chen, Yan Dan Lei, Zhao Bin, Ben Choi Yeung and Yuan Xiaojun., " A 18mW Tx 22mW Rx Tranceiver for 2.45GHz IEEE 802.15.4 WPAN in 0.18- µm CMOS ", IEEE A-SSCC, Dig. Tech. Paper,Nov. 2010.

[2] "Theory and Application of Passive SAW Radio Transponders as Sensors", IEEE Tras on Ultrasonics, Ferroelectronics and frequency control, Vol. 45, NO. 5, Sep 1998

[3] W.C Wilson & P.D. Juarez, "Emerging Needs for Pervasive Passive Wireless Sensor Networks on Aerospace Vehicles" Sciencedirect, 2014

[4] V. Kuhn et. Al. ,"A Multi-Band Stacked RF Energy Harvester with RF-to-DC Efficiency Up to 84%" IEEE Transactions on MTT, May 2015

★★★